Indian Journal of Science and Technology, *Vol 7(2), 123–134, February 2014*
ISSN (Print): 0974-6846
ISSN (Online) : 0974-5645

Effects of Dy_2O_3 Nanoparticle Addition on Structural and Superconducting Properties of BSCCO

Amir Zelati[1*], Ahmad Amirabadizadeh[1], Ahmad Kompany[2], Hadi Salamati[3] and Jeff Sonier[4]

[1]Department of Physics, University of Birjand, Iran; a_zelati@yahoo.com, ahmadamirabadi@yahoo.com
[2]Department of Physics, Ferdowsi University of Mashhad, Iran; Kompany@ferdowsi.um.ac.ir
[3]Faculty of Physics, Isfahan University of Technology, Iran; salamati@cc.iut.ac.ir
[4]Depatment of Physics, Simon Fraser University, Burnaby, BC, Canada; jeff Sonier: jsonier@sfu.ca

Abstract

To study the effects of Dy_2O_3 nanoparticle addition to BSCCO superconducting system, four bulk polycrystalline samples with general formula of $Bi_{1.6}Pb_{0.4}Sr_2Ca_2Cu_3O_y + xDy_2O_3$ (where, x = 0.0, 0.5, 1.0, 2.0 wt%) were prepared by chemical sol-gel method. Dy_2O_3 nanoparticles were added to the BSCCO system in order to improve the connectivity among the grains leading to increase in the critical current density (J_c). X-ray diffraction, SEM, TEM and Energy Dispersive X-ray spectroscopy (EDX) were used for structural characterization of the samples. XRD analysis showed that both (Bi,Pb)-2223 and Bi-2212 phases coexist in the samples having orthorhombic crystal structure. DC electrical resistivity and AC magnetic susceptibility were measured. DC electrical resistivity and AC magnetic susceptibility measurements showed improvements in ΔT_c ($T_{c,\,onset}$-$T_{c.\ R=0}$), hole concentration, intergrain connectivity and J_c in BSCCO superconducting system by adding 0.5 wt% Dy_2O_3 nanoparticles to it. While for x > 1, DC and AC measurements did not present satisfactory results.

Keywords: AC Magnetic Susceptibility, Bi-2223, DC Electrical Resistivity, SEM, TEM, XRD

1. Introduction

Since the discovery of Bi-based superconducting systems, a great amount of work concerning preparation, superconducting properties, and the structure of these compounds has been done[1–3]. The BSCCO system, mainly contains three phases in the general formula $Bi_2Sr_2Ca_{n-1}Cu_nO_{2n+4+y}$ where, n = 1, 2 and 3 refers to the number of CuO_2 layers which yields 10, 95 and 110 K superconducting phases, respectively[4]. The Bi-2201, Bi-2212 and Bi-2223 phases have single, double and triple layers of CuO_2 in the sub-unit cell, respectively. It is believed that in BSCCO system more CuO_2 planes is associated with higher value of T_c (R = 0)[5,6]. The superconducting properties of BSCCO system can be controlled by addition or substitution of elements. The enhancement or destruction of the superconducting properties depends on the characteristics of the dopant in the crystal structure. Pb is the most important substituting element that influences the microstructure, phase composition, and the related superconducting properties of BSCCO system. The presence of Pb in the initial mixture favors the reaction kinetics of Bi-2223 phase[7,8]. Pb addition results in the creation of a superconducting solid solution $Bi_{2-x}Pb_xSr_2Ca_2Cu_3O_d$ by partial substitution of bismuth and the optimum Pb content (x) lies between 0.3 and 0.4, so x = 0.4 was selected for preparing the samples in this report[9,10]. Despite many efforts to obtain Bi-2223 single phase, preparation of BSCCO systems normally leads to the coexistence of (Bi,Pb)-2223 and Bi-2212 phases in the samples.

In the application of the BSCCO superconductors, higher critical current density (J_c) has a more significant role than the other factors. However, the major limitations of the BSCCO superconductor applications are the

*Author for correspondence

intergrain weak links and weak flux pinning capability, which leads to weak critical current density in bulk samples. There have been remarkable improvements in enhancing transport properties of this high-T_c superconductor, since BSCCO superconductor was discovered. We can enhance the superconducting properties of BSCCO system by addition or substitution of elements with different ionic radius and different bonding characters. As an example, to obtain more applicable BSCCO sample we can add or substitute metallic elements to the BSCCO system to improve the connectivity between grains leading to higher J_c[11]. Several researchers[12–16] have investigated the effects of rare earth oxides and some other oxides substitution or addition on the superconducting and structural properties of BSCCO system. The works of most of these researches are related to addition or substitution of micro-oxide powders to BSCCO systems.

With nano technology developments, a wide range of nanostructure materials has been synthesized. In the nano size range, the particles have a high proportion of atoms located at its surface as compared to bulk materials, giving rise to unique physical and chemical properties that are very different from their bulk counterparts[17]. In recent years, studying the effects of nanoparticles addition or substitution to BSCCO system has been of much interest [18–21]. When nanoparticles are added to the BSCCO system, due to the tiny size of nanoparticles, they settle easier and much more among the grains of these ceramic superconductors than the micro size dopant. If adequate amount of nanoparticles with metallic character is added to the BSCCO, the intergrain connectivity will possibly improve.

In this study, we added Dy_2O_3 nanoparticles to the BSCCO system to improve the connectivity between grains. We generally expect that a small amount of Dy nanoparticles addition in BSCCO system would enhance connectivity between the grains due to metallic character of Dy, or would make possible pinning centers between grain boundaries. The general formula for preparing the samples of this research was $Bi_{1.6}Pb_{0.4}Sr_2Ca_2Cu_3O_y + xDy_2O_3$ and x = 0.0, 0.5, 1.0, 2.0 wt%. To the best of our knowledge, the previous studies on the effects of Dy on BSCCO system were related to micro size of dysprosium powder and were focused on the magnetic properties. Berger et al.[16] studied coexistence of ferromagnetism and high-T_c superconductivity in micron doping of Dy on BSCCO system but the structural effect of this dopant has been left untouched. The BSCCO sample was prepared by chemical sol-gel method[22–24] and Dy_2O_3 nanopowder by combustion method. XRD, SEM, TEM, EDX and SAED were used for morphological and structural characterization of the prepared samples. DC resistivity measurements and AC magnetic susceptibility measurements were performed to study the superconducting properties of the samples and to achieve the optimum amount of Dy nanoparticle addition to the BSCCO system.

2. Experimental

2.1 Sample Preparation

The samples were prepared according to the general formula $Bi_{1.6}Pb_{0.4}Sr_2Ca_2Cu_3O_y + xDy_2O_3$ and x = 0.0, 0.5, 1, 2 wt% on three steps as follows:

Step 1: BSCCO sample with chemical composition $Bi_{1.6}Pb_{0.4}Sr_2Ca_2Cu_3O_y$ was prepared by chemical sol-gel method, using the powders of $Bi(NO_3)_2.5H_2O$, $Pb(NO_3)_2$, $Sr(NO_3)_2$, $Ca(NO_3)_2.4H_2O$ and $Cu(NO_3)_2.3\ H_2O$, as the starting materials. EDTA with chemical composition $N_2H_{10}O_{16}$ was used as the complexing agent with the molar ratio: EDTA/cation = 1, Ethylene Glycol (EG) with chemical composition $C_2H_4(OH)_2$ as the binding agent of complexes with the molar ratio: EG/cation = 3 and urea as the fuel with the molar ratio: urea/cation = 0.7. Distilled water and nitric acid were used as the solvent. Bismuth nitrate was poured in appropriate volume of distilled water (400 mL for 40 gr final production) at temperature 40°C. The certain amount of nitric acid was added to the mixture to make the Bismuth solution. Then the other nitrates were added to this solution. After stirring the mixture, a transparent blue solution with pH = 1 was obtained, which we named the material solution. After that the certain amount of EG was solved in appropriate volume of distilled water (400 mL for 50 gr final production) at temperature 40°C and then EDTA was added to this solution which resulted in the formation of precipitation. In order to annihilate the precipitation, NH_3OH was added to the liquid mixture so that a transparent solution with pH = 6, was obtained (main solution). The material solution was poured in to the main solution drop by drop at temperature 60°C until the starting the formation of the precipitation. At this time, the process of adding the material solution to the main solution was stopped to eliminate the precipitation via NH_3OH. This process was repeated until all the material solution was added to the main solution and obtaining the gel with pH = 4. The next

performance was adding urea, as the fuel to the prepared gel. Then, the urea added gel was dried on a hot plate with gradually increasing temperature from 60 to 200°C, which took 3 days to complete the process of drying. At the end of this time a rather weak combustion occurred and a grey color powder was produced. The powder was grinded and calcined at 850°C for 7 h in air. After calcination a black powder obtained. The prepared powder was then grinded and divided to 4 segments.

Step 2: Dy_2O_3 nanoparticles were prepared by combustion method using, Dysprosium (III) Nitrate Pantahydrate with chemical composition $Dy(NO_3).5H_2O$ as starting material. Distilled water was used as the solvent and glycine with chemical formula $C_2H_5NO_2$ as the fuel of the reaction. Dysprosium (III) Nitrate Pantahydrate was solved in adequate amount of distilled water. After obtaining aqueous solution of cation, Dy^{3+}, glycine as the fuel for combustion was added to the solution. The liquid mixture was placed inside the pre-heated (300°C) oven for one hour. Combustion took place inside the oven and russet smoke of the NO_2 gas came out. The resultant product was a voluminous, foamy white powder. Later, XRD pattern and TEM images confirmed the cubic structure and the nano-size of the prepared Dy_2O_3 powder.

Step 3: Dy_2O_3 nanopowder, in this step, added to each of segments (1, 2, 3 and 4) prepared in the first step with 0.0, 0.5, 1.0 and 2.0 wt%, respectively. Each sample was grinded and calcined at 850°C for 7 h in air. The calcined powders were grinded again and pressed under 450 MPa pressure to form pellets with 11mm diameter and 3.5 mm thick. The prepared pellets were finally sintered at 860°C for 24 h in air. Sample with x = 0.0 in general chemical formula, $Bi_{1.6}Pb_{0.4}Sr_2Ca_2Cu_3O_y + xDy_2O_3$, was labeled as sample 'A' and the other samples labeled as 'B' (x = 0.5), C (x = 1.0) and D (x = 2.0).

2.2 Sample Characterization

XRD, SEM, TEM, EDX and Selected Area Electron Diffraction (SAED) were used for the structural studied of the samples. DC resistivity (R-T) and AC magnetic susceptibility measurements were carried on to study the superconducting properties of the samples. The X-ray powder diffraction pattern for each sample was obtained using CuKα (1.54Å) radiation in the range 2θ = 20–65° by a Rigaku R-Axis Diffractometer. Phase purity and the lattice parameters were obtained from these patterns. SEM and TEM imaging were used to examine the surface morphology and grain structure of the samples and EDX was applied for the elemental analysis of the samples.

SEM images were taken by using a Strata Dual beam 235 field emission Scanning Electron Microscope. TEM images, EDX spectra and SAED patterns were obtained by using a TecnaiG2 Scanning Transmission Electron Microscope (STEM). The R–T behavior of the samples from 30 K to room temperature was investigated in order to determine the superconducting transition temperature. The electrical resistance was measured by the standard four-probe method. The magnetic susceptibility measurements carried out employing a Quantum Design SQUID magnetometer MPMS-XL7 that works between 1.8 and 400 K with a 7 Tesla superconducting magnet. Diamagnetic corrections were applied for the sample holder and the core diamagnetism of the samples.

3. Results and Discussion

3.1 X-ray Diffraction and Microstructure Studies

XRD patterns of $Bi_{1.6}Pb_{0.4}Sr_2Ca_2Cu_3O_y + xDy_2O_3$ (x = 0.00, 0.5, 1 and 2 wt%) samples indicated that all samples two phases, Bi-2212 and Bi-2223 phases (Figure 1). A weak impurity phase Ca_2PbO_4 peak at 2θ = 32° was identified in samples 'C' and 'D'.

The XRD patterns revealed that all the samples consist of (2212) and (2223) phases, with (2223) phase the dominant. To estimate the volume fraction of the present phases, we used the corresponding Bi-2212 and Bi-2223 peaks, and the following formulas[24]:

$$B_i - (2223)\% = \frac{\Sigma I(2223)}{\Sigma I(2223) + I(2212) + I(Ca_2PO_4)} \times 100$$

$$B_i - (2212)\% = \frac{\Sigma I(2212)}{\Sigma I(2223) + I(2212) + I(Ca_2PO_4)} \times 100$$

where, $I(2223)$, $I(2212)$ and $I(Ca_2PO_4)$ are the intensities of the (hkl) XRD peaks for Bi-2223, Bi-2212 and the impurity Ca_2PO_4 phases, respectively. The calculated relative portions of each phase of the samples are listed in Table 1. As seen in the table, samples with x = 0.0, 0.5, 1.0 and 2.0 contained 76%, 71%, 64% and 62% of the 2223 phase, respectively. In addition, increasing the amount of the additive into our samples resulted in a decrease in the intensities of the peaks of the 2223 phase. The percentage of the 2223 phase did not change that much in sample B comparing to sample A so it can be said that adding 0.5 wt% Dy nanoparticle to the BSCCO system almost

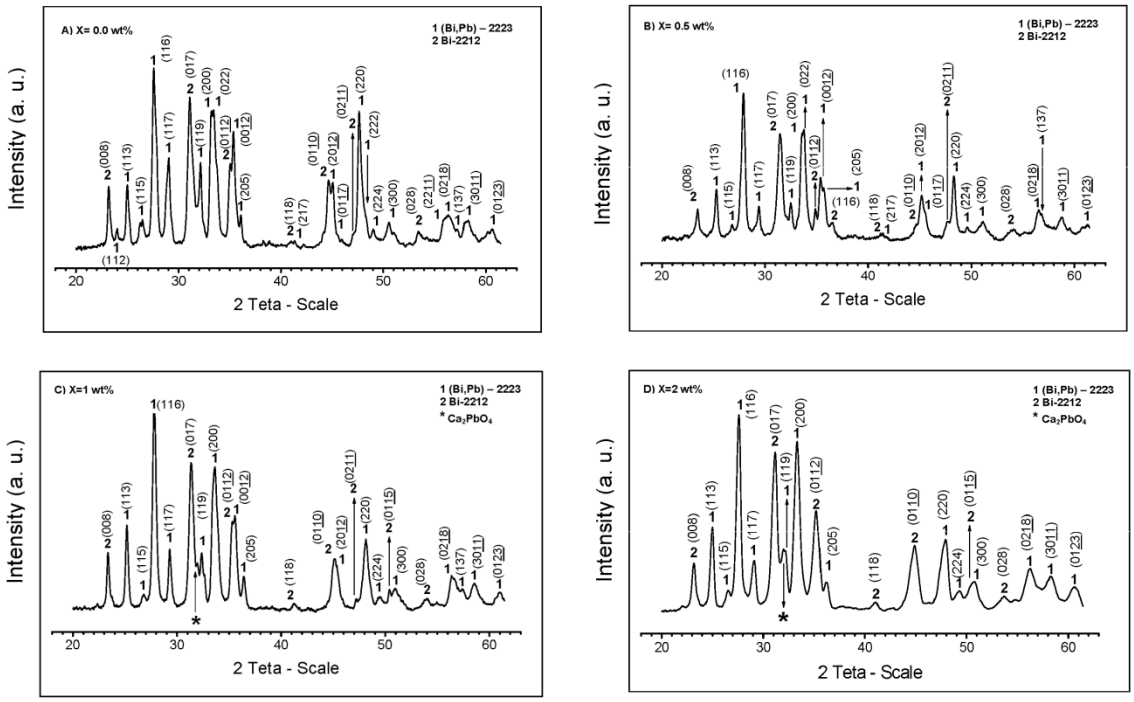

Figure 1. XRD patterns of $Bi_{1.6}Pb_{0.4}Sr_2Ca_2Cu_3Oy + xDy_2O_3$ samples, A) x = 0.0, B) x = 0.5, C) x = 1.0 and D) x = 2.0 wt%. Peaks of (Bi,Pb)-2223 and Bi-2212 phases are indexed 1 and 2, respectively.

Table 1. The lattice parameters and percentage volume fraction of Bi-2223 and Bi-2212 phases in $Bi_{1.6}Pb_{0.4}Sr_2Ca_2Cu_3Oy + xDy_2O_3$ (x = 0.0–2.0) samples.

Sample	Orthorhombic unit cell (Bi-2223 phase)			Volume fraction of phase formed (%)	
	a(Å)	b(Å)	c(Å)	Bi-2223 phase	Bi-2212 phase
A	5.315	5.419	37.289	76	24
B	5.313	5.422	37.292	71	29
C	5.309	5.418	37.279	64	32
D	5.305	5.417	37.266	62	33

did not reduce the amount of 2223 phase. The percent amounts of the 2223 and 2212 phases as a function of x evaluated from the XRD patterns of $Bi_{1.6}Pb_{0.4}Sr_2Ca_2Cu_3O_y + xDy_2O_3$ (x = 0.0, 0.5, 1.0 and 2.0) samples are given in Figure 2.

The crystal system of Dy-free sample was found to be orthorhombic with the lattice parameters of a = 5.315Å, b = 5.419Å and c = 37.298Å. Almost, the same lattice parameters were obtained for the Dy nanoparticles-added samples. The results are given in Table 1. There is no distortion in the crystal system of the Dy-added Bi-2223, which shows that Dy particles do not participate in the crystal structure of the Bi-2223. Therefore, as we expected the added nanoparticles are sited between the superconducting grains. Either the role of such nanoparticle impurities can act as the pinning centers to fix vortices or they may enhance connectivity among the grains, which leads to higher J_c[11].

Figure 3 displays the surface SEM images of the Dy nanoparticles-free and -added samples. It is observed that the microstructures of all samples exhibit a common feature of plate-like grains and are randomly distributed. We believe that white particles sited between the grains are Dy nanoparticles, which are obvious in the micrographs of Dy-added samples. These particles can enhance the connectivity among the grains and they can increase the pinning centers to fix the vortices. The SEM results corroborate well with the XRD results. In addition to

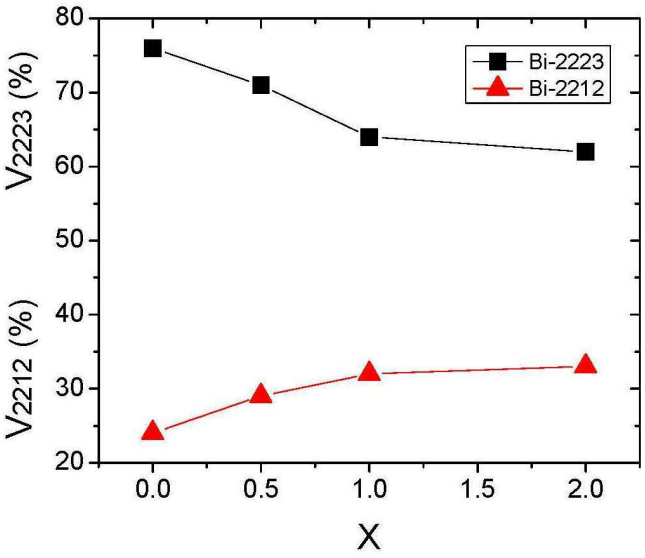

Figure 2. Volume fraction of Bi-(2223) and Bi-(2212) phases determined from XRD patterns.

the intergranular distribution of the nanoparticles, the presence of the nanoparticles can be observed in the other parts of microstructure of Dy added samples. A decrease in the grain size is observed for samples C and D that may reduce superconducting properties of the BSCCO system.

TEM images and EDX spectra from the powders of the Dy nanoparticles-added samples are presented in Figure 4. TEM images show that the grains are micro sized, which is essential BSCCO as a ceramic superconductor. Furthermore, the presence of the Dy nanoparticles can be clearly observed close to the grain boundaries. EDX was utilized to confirm the chemical compositions of the synthesized samples especially for the Dy-added samples. As shown in Figure 4, Ca, O, Cu, Dy, Pb, Bi and Sr peaks are presented in Dy-added samples. The morphology and size distribution of the Dy_2O_3 nanoparticles prepared for this work are shown in Figure 5.1 The TEM image of the sample confirms the nano-size of the particles in the

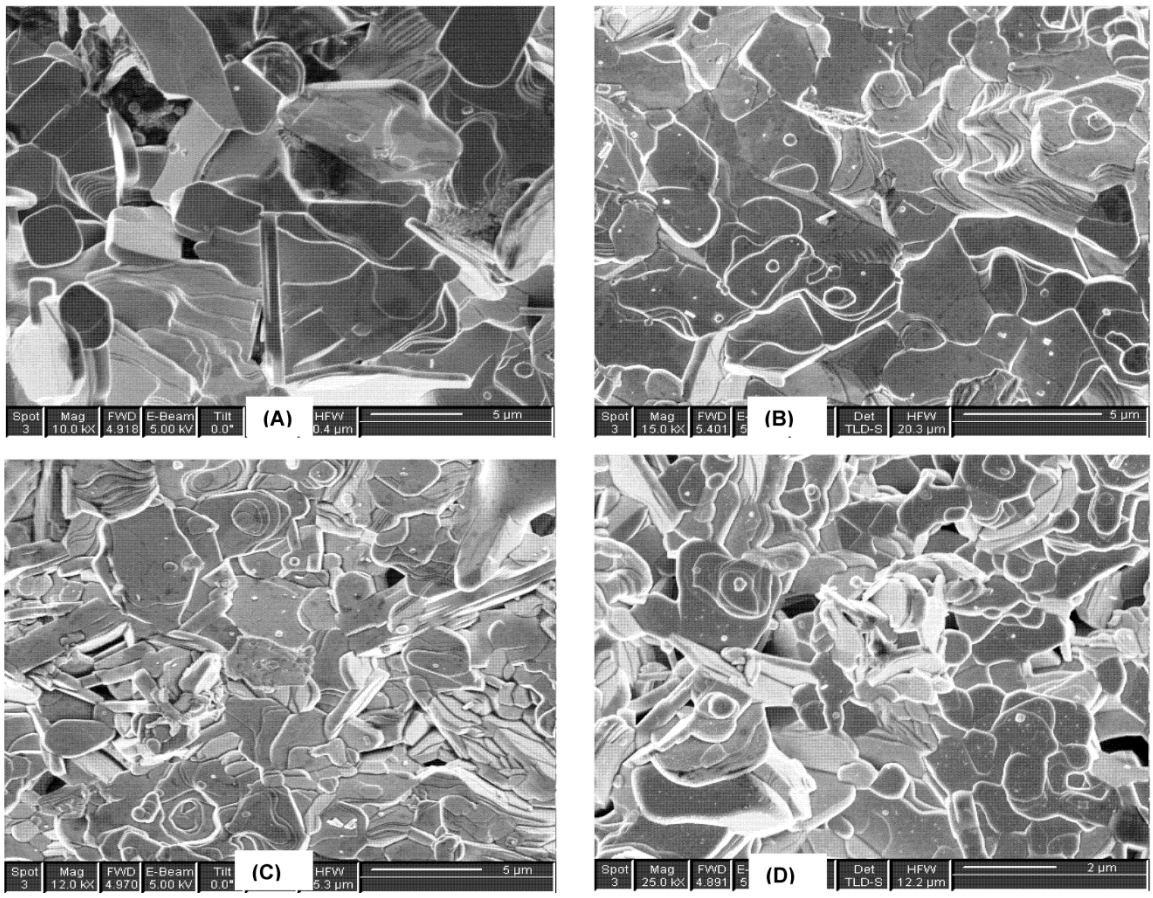

Figure 3. SEM surface micrographs of $Bi_{1.6}Pb_{0.4}Sr_2Ca_2Cu_3Oy + xDy_2O_3$ samples, A) x = 0.5, B) x = 0.5, C) x = 1 and D) x = 2 wt%.

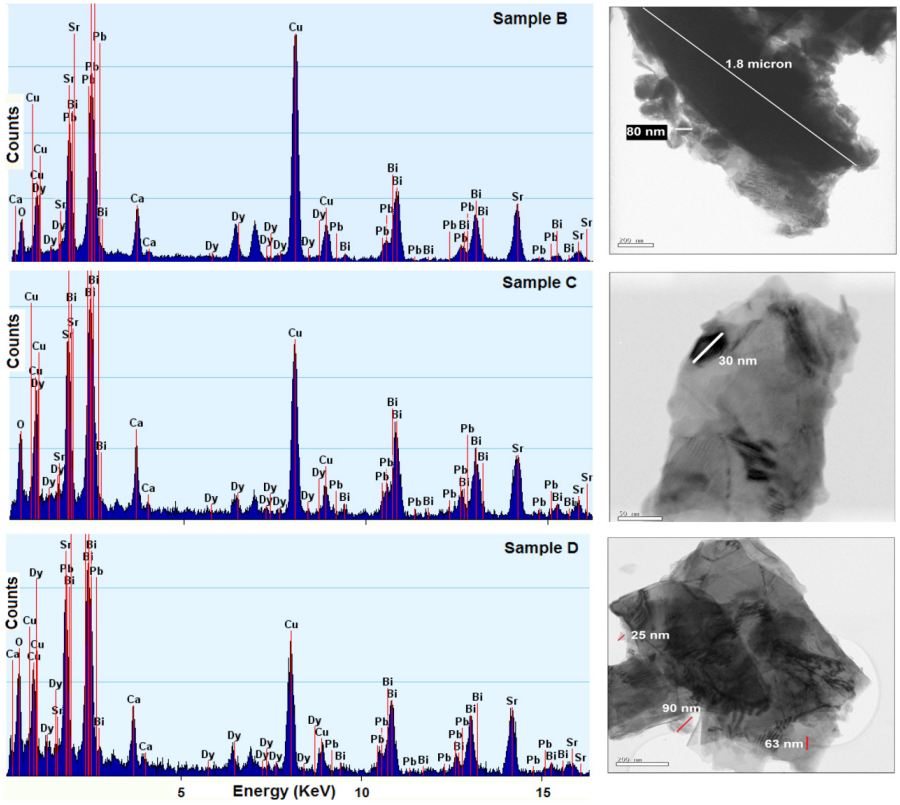

Figure 4. TEM images and EDX spectra of the powders $Bi_{1.6}Pb_{0.4}Sr_2Ca_2Cu_3Oy + xDy_2O_3$ samples, B) x = 0.5, C) x = 1.0 and D) x = 2.0.

range of 10–90 nm. The histogram shows that the average particle size of Dy_2O_3 sample is about 28 nm.

SAED patterns of Dy-free sample taken along the [100] and [001] zone-axis directions of orthorhombic crystal, respectively, are shown in Figure 5.2 (a)–(b). Since for the other samples there is not any significant variation in the SAED patterns, only SAED patterns for Dy-free sample are shown. The ratio of the lattice parameter b/a based on these patterns is about 1.02, which is close to the value obtained by the XRD results[25,26]. Indexing of the two important planes has been elucidated in diffraction pattern.

The theoretical density of BPSCCO system is about 6.3 g/cm^3 obtained from the lattice parameters[27]. The density of pellets in this work was determined as 5.48, 5.19, 4.87 and 4.71 g/cm^3 for x = 0.0 to x =2.0, respectively, measured by water displacement Archimedes' method. The bulk densities obtained by Archimedes technique is in the range of 75 to 87% of the theoretical values. This result is in accordance with the porous structure of ceramic superconductors.

3.2 Superconducting Properties Measurements

As shown in Figure 6, DC electrical resistance (R–T) reveals that the resistivity of the presented samples decrease linearly with temperature in the normal state. All samples displayed a metallic character above onset temperature, which is defined as the temperature where R–T plot deviates from linearity[10]. Derivatives of the R–T curves were calculated to obtain the zero onset transition to the superconducting state. The plots of samples A, B and C have a shoulder, which we believe to be due to the coexistence of Bi-2223 and Bi-2212 phases with considerable ratio. The plots show that the onset temperatures T_c (onset) of the samples A and B are in the close vicinity of 109.5 K. T_c (onset) for samples C and D are about 106 and 101, respectively. The zero resistivity critical temperature T_c (R = 0) for Dy-free sample, A(x = 0.0), was 76.5 K. The transition temperature width (ΔT_c) of the sample D with x = 2.0 was narrower than those of the other samples were. But since the T_c (onset) for sample D is the lowest, the DC

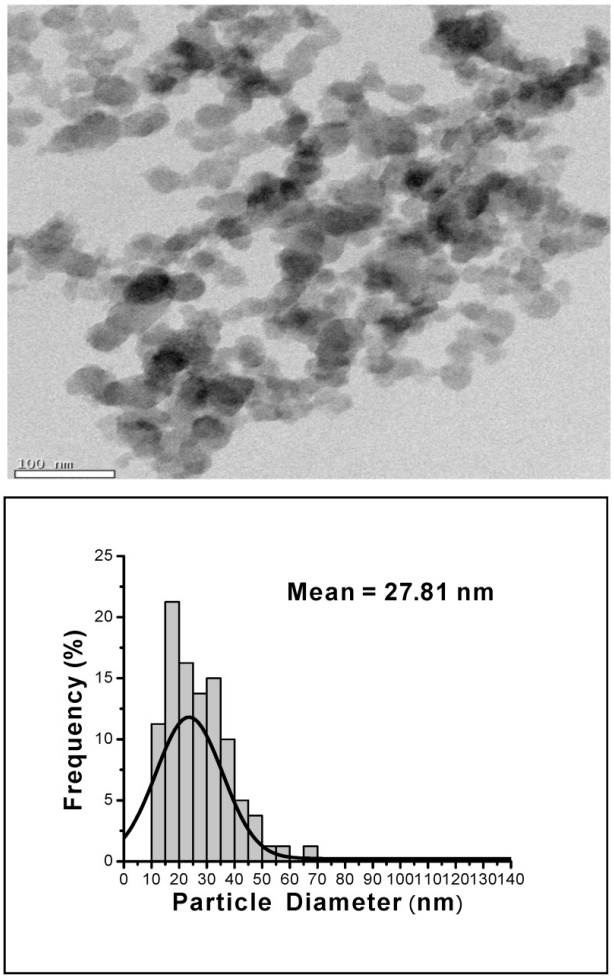

Figure 5.1. TEM image and histogram of Dy_2O_3 nanoparticles.

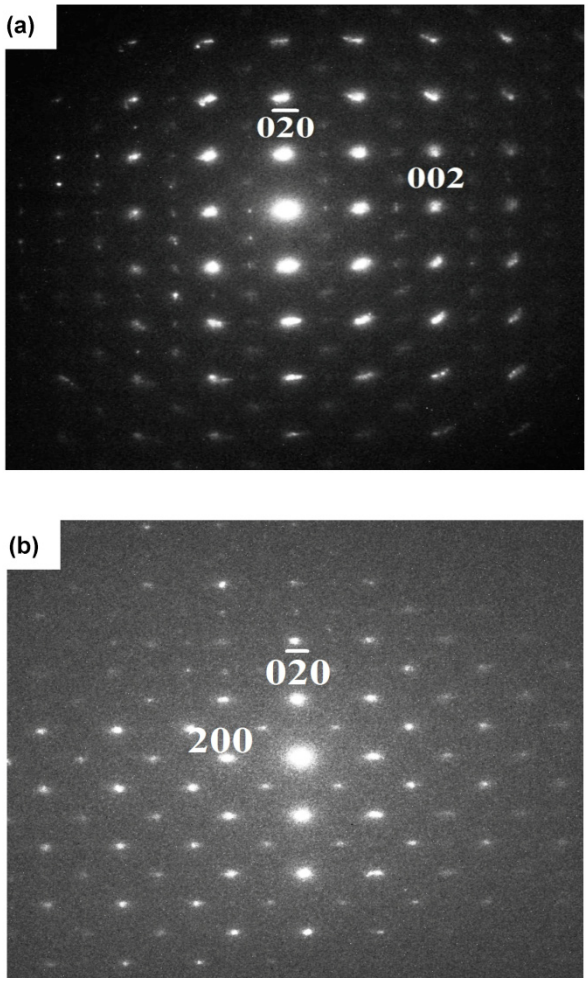

Figure 5.2. Electron diffraction patterns of the orthor hombic $Bi_{1.6}Pb_{0.4}Sr_2Ca_2Cu_3Oy$ (a) [100], (b) [001].

electrical resistance measurement doesn't show a good result for this sample. ΔT_c shows lower amount for sample B comparing to sample A, which means inter-grain connectivity is enhanced in sample B[28]. It means that 0.5% Dy nanoparticles addition to the BSCCO system resulted in decreasing of ΔT_c and increasing of inter-grain connectivity, which consequently increase intergranular J_c. This result is in a good agreement with the XRD and SEM results, because the percentage of the 2223 phase is almost the same in sample A and B, while 0.5 wt% added Dy nanoparticles to BSCCO system enhance the connectivity between the grains. DC measurements results for samples C and D were not as good as the results for sample B. The percentage of the 2223 phase in samples C and D reduced more than 12% comparing to the percentage of the 2223 phase in sample A. In addition, a decrease in the grain size was observed in SEM images of samples C and D, which caused a reduction in their superconducting properties. T_c (R = 0) in $Bi_{1.6}Pb_{0.4}Sr_2Ca_2Cu_3Oy + xDy_2O_3$ (x = 0.0–2.0) samples are tabulated in Table 2. The variation of T_c with Dy content, x, is given in Figure 7.

A relationship holds between the superconducting transition temperature and the hole concentration *p*. The carrier concentration *p* is calculated, using the relation given below[29]:

$$p = 0.16 - \left[\left(1 - T_c / T_c^{\max}\right)/82.6\right]^{1/2}$$

where, $T_c^{\max}$ is taken as 110 K for the Bi-2223 system. Previous calculations for the un-substituted Bi-2223 had shown that the values of p are in the range of 0.116 to 0.160. Figure 8 shows the critical temperature versus hole concentration plot. Hole carrier concentration varies from 0.0962 for sample C to 0.1026 for sample B. The hole

concentration is 0.0962 and 0.1007 for samples A and D, respectively. The highest hole concentration is observed in sample B with x = 0.5%. Based on the results of the Figures. 6–8 sample B shows better electrical characteristic in the comparison with the others.

AC susceptibility measurement ($\chi' + i\,\chi''$) is widely used as a nondestructive method for determination and characterization of the intra-grain and inter-grain features of the high temperature superconductors. The in-phase component of fundamental susceptibility, χ', shows two significant drops as the temperature is decreased below T_c for granular superconductors. The sharp drop, near T_c, corresponds only to the intrinsic properties of the grains. Another drop at low temperatures indicates gradual changes associated with the occurrence of bulk superconductivity, where superconducting current flow from grain to grain. The out-of-phase component, χ'', generally exhibits a peak with decreasing temperature below T_c, which is attributed to the absorption of magnetic energy of the superconductor from the AC field. Therefore, χ', is proportional to an amount of flux penetration into the body of the superconductor, while χ'' is associated with AC losses in the mixed state of superconductor[11].

Table 2. The critical temperatures $T_{c,zero}$ (K), $T_{c,onset}$ (K), ΔT_c (K) and mass density of $Bi_{1.6}Pb_{0.4}Sr_2Ca_2Cu_3O_y + xDy_2O_3$ samples

Sample	Dy (x)	T_c (onset) K	T_c (R=0) K	ΔT_c K	Mass density (g/cm^{-3})
A	0.0	109.5	76.5	33	5.48
B	0.5	109.5	80	29.5	5.19
C	1.0	106	73	33	4.87
D	2.0	101	78	23	4.71

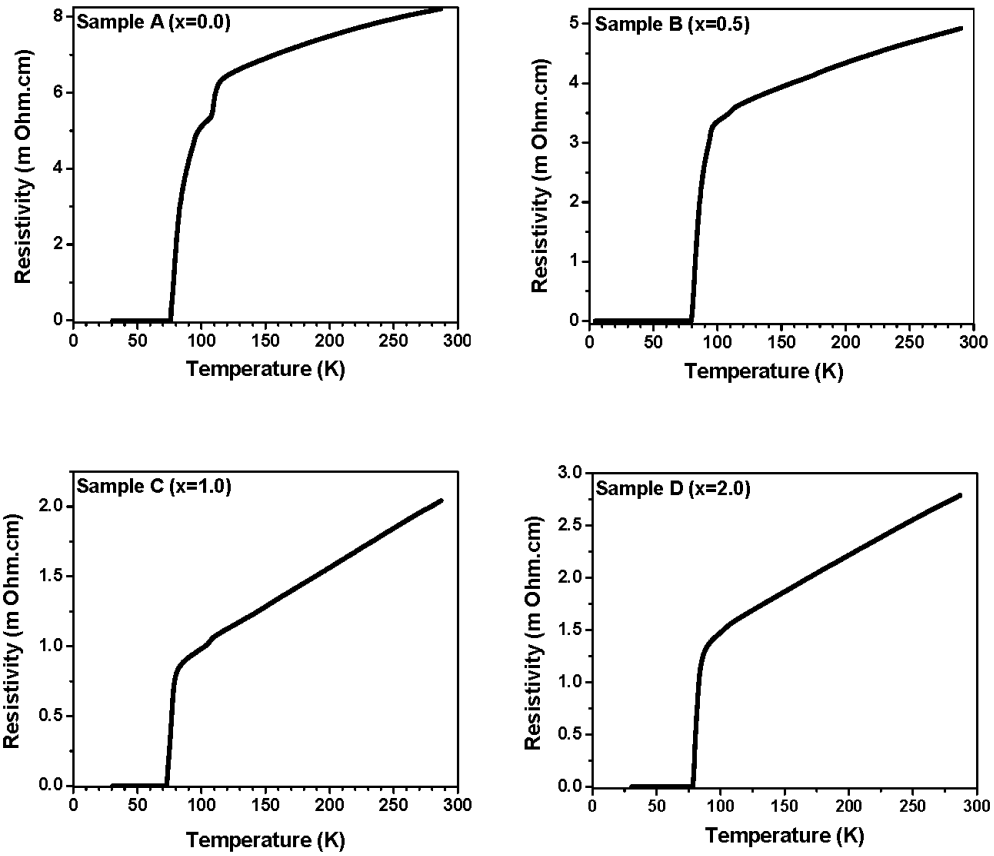

Figure 6. Temperature dependences of the electrical resistivity for $Bi_{1.6}Pb_{0.4}Sr_2Ca_2Cu_3Oy + xDy_2O_3$ samples, A) x = 0.5, B) x = 0.5, C) x = 1 and D) x = 2.

In Figure 9, the measurements of susceptibility versus temperature for Dy nanoparticles-free and Dy nanoparticles-added samples have been plotted for AC field of 80 A/m with f = 330 Hz. A broad magnetic transition for samples A (x = 0.0) and D (x = 2.0) are observed. However, samples B (x =0.5) and C (x = 1.0) have a slightly sharper transition compared to sample A and D. These results suggest that B and C samples have better inter-granular coupling between the grains, which is in good agreement with DC electrical resistivity measurements. It is seen that there are 2 peaks for χ'', which we believe is related to the coexistence of Bi-2223 and Bi-2212 phases. The first peak (at higher temperature) of imagery part of AC susceptibility, χ'', for samples A, B, C and D is sited at temperature about 99, 77, 87 and 97.5 K, respectively. It means that for samples A, B, C and D, AC losses start at 99, 77, 87 and 97.5 K, respectively, so for sample B with x = 0.5% AC loss starts at lower temperature comparing to the other samples. The curve obtained from derivation of the χ' versus temperature is inserted in Figure 9, displaying intra- and intergrain superconducting transition temperatures. The intra-grain transition temperature was determined to be about 100 K for all samples. However, the inter-grain transition temperature for sample A, B, C and D is 75, 73, 80 and 70, respectively.

Figure 10 shows the AC susceptibility curves of the prepared bulk samples measured in the presence of several magnetic field values. The diamagnetic onset temperature of the superconducting transition is about 100 K for all samples. This temperature is independent of the applied field values for Dy nanoparticles-free and -added polycrystalline samples. It is well known that the minimum full flux penetration field, H_p, becomes larger by decreasing temperature from T_c to the temperature T_p,

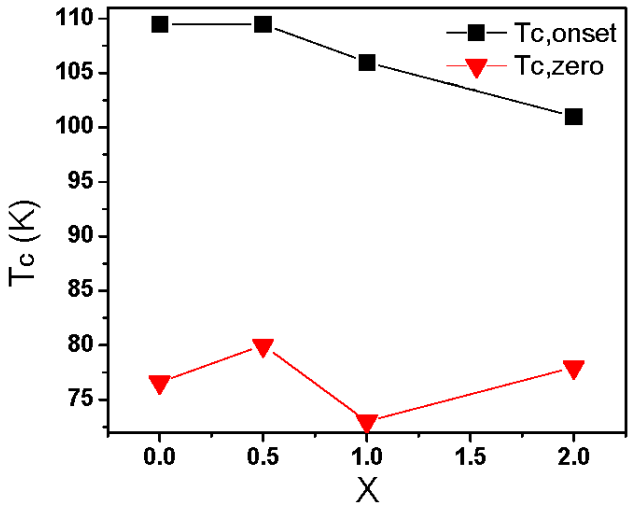

Figure 7. Variation of critical temperature of $Bi_{1.6}Pb_{0.4}Sr_2Ca_2Cu_3Oy + xDy_2O_3$ (x = 0.0–2.0) samples.

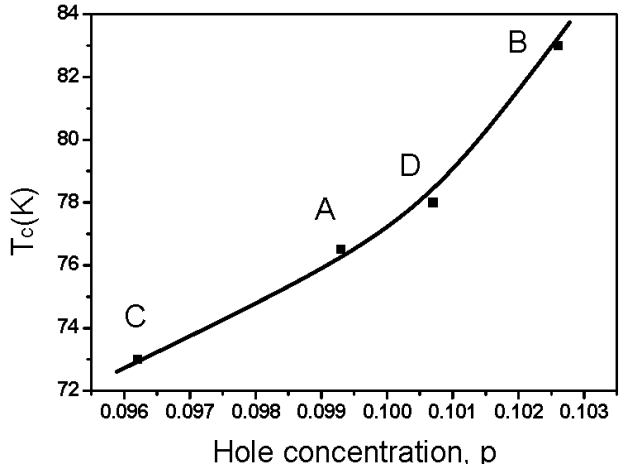

Figure 8. Superconducting transition temperature versus hole concentration of Dy-free and Dy-added samples A) x = 0.0, B) x = 0.5, C) x = 1.0, and D) x = 2.0.

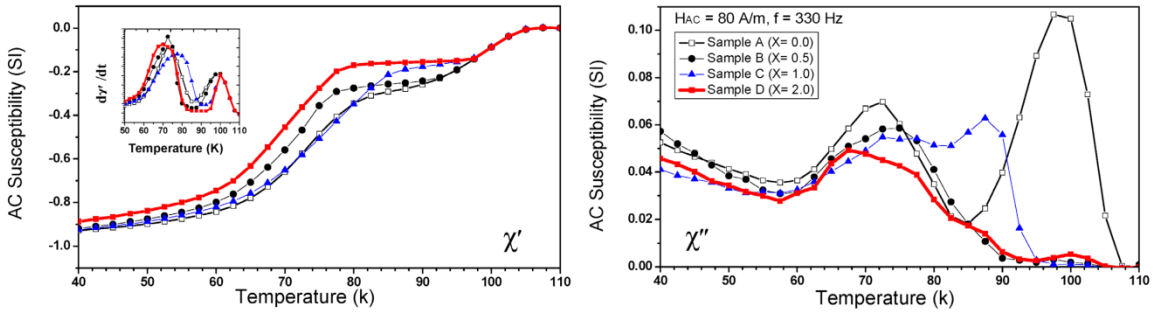

Figure 9. AC magnetic susceptibility as a function of temperature for all samples χ') Real part, χ'') Inset Image: derivation of in-phase component versus temperature.

at which χ'' peaks occur. The value of the measured AC field at these temperatures is sufficiently large enough to penetrate to the center of the sample. When $H_{AC} = H_p$, the full flux penetration occurs. A function of the form $H_p = H_{AC}(1-t)^n$ fits best the data obtained, where, $t = (T/T_c)$ is the reduced temperature. The function obtained thereby is employed as a scaling function for temperature sweep measurements and it is most accurate at temperatures near T_c. By fitting H_{AC} versus $(1-t)^n$ plot, we have found n = 2.3 for our samples. Figure 11 shows the temperature dependence of the intergranular critical current density, J_c calculated from H_p values. According to Bean's model[11,30] J_c at the peak temperature, T_p can be calculated using the following relation:

$$J_c(T_p) = H_p / R \approx H_p / \sqrt{ab}$$

where, $2a_*2b$ is the cross-section. As shown in Figure 11, comparing to all samples, J_c shows the best result in sample B (x = 0.5). It means that adding 0.5 wt% Dy nanoparticles to BSCCO system causes a great improvement in J_c. There is also a quite good improvement in J_c for sample C (x = 1.0).

Based on the results of Figures 9–11, the optimum amount of Dy nanoparticles addition to the BSCCO system is x = 0.5 wt%. In this amount, while Bi-2223 phase remains almost unchanged comparing to the Dy-free sample, nanoparticles settle between the grains and the grains connectivity is increased. For 0.5 < x < 1 a fair improvement can also be observed in inter-grain connectivity and intergranular J_c but the greater amount of Dy nanoparticles addition (x > 1) cause a destruction in the superconducting properties.

4. Conclusion

The samples with nominal composition $Bi_{1.6}Pb_{0.3}Sr_2Ca_2Cu_3 + xDy_2O_3$ were prepared by the chemical sol-gel method. X-ray diffraction indicated that both Bi-2223 and Bi-2212 phases coexisted with considerable ratios in the samples but Bi-2223 held the dominant phase. The volume fraction, which was estimated by XRD peaks intensities, showed that the Dy nanoparticle-free sample had the

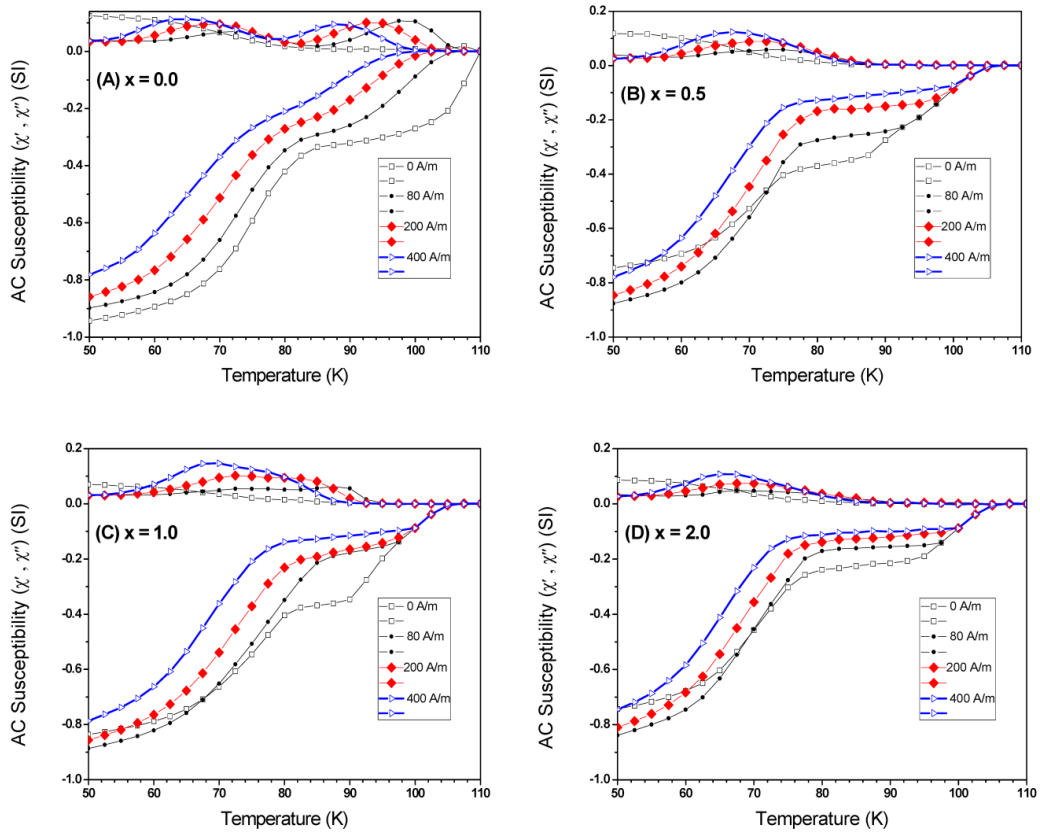

Figure 10. AC magnetic susceptibility as a function of temperature for Samples A, B, C and D.

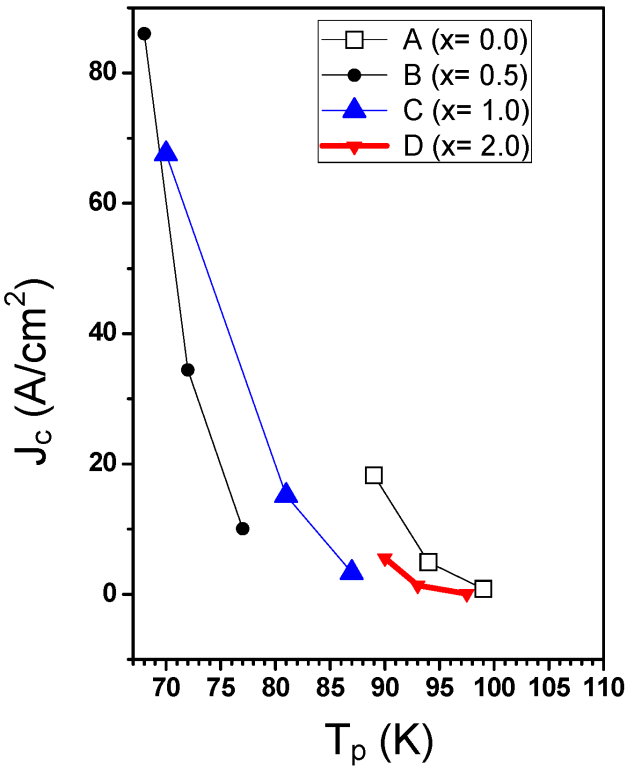

Figure 11. Variation of critical current density with temperature.

highest volume fraction of the Bi-2223 high-T_c phase. Sample with 0.5 wt% added Dy nanoparticles had almost the same volume fraction of the Bi-2223 phse as Dy-free sample. SEM results showed that the added Dy nanoparticles settled among the grains boundaries and indicated that the grains sizes were reduced in samples with x > 0.5 wt%. Based on XRD and SEM results, while sample B(x = 0.5) kept Bi-2223 phase almost untouched, it increased the connectivity among the grains by settling nanoparticle between the grains boundaries. Based on electron diffraction results the ratio of the lattice parameter b/a was estimated about 1.02, which is very close to the value obtained by the XRD results. EDX confirmed the presence of the desired elements in the chemical composition of the samples. DC electrical resistivity measurements showed a narrow ΔT_c for sample with x = 0.5 wt%, which means this sample had the best intergrain connectivity. $T_{c,\ onset}$ and $T_{c,R\ =\ 0}$ for sample with x = 0.5 wt% were obtained 109.5 and 80K, respectively. Hole concentration of the samples, calculated by the results of DC measurements, showed the highest amount in sample with x = 0.5 wt%. Intergranular coupling, intra- and inter-grain transition temperatures and intergranular critical current density, J_c, were calculated by AC magnetic susceptibility measurements. AC measurements demonstrated the best improvements, especially in J_c, for sample with x = 0.5 wt%, which is in a good agreement with DC measurements, XRD and SEM. The optimum amount of Dy nanoparticle addition to the BSCCO system was x = 0.5 wt%. While for x > 1, DC and AC measurements, XRD and SEM did not present satisfactory results.

5. Acknowledgement

The authors would like to thank 4D labs, Simon Fraser University (SFU) for helping us with the all the related measurements and our special appreciation goes to Prof. Karen Kavanagh, Dr. Omid Salehzadeh Einabad and Dr. Wendell Huttema.

6. References

1. Maeda H, Tnaka Y, Fukutomi M, Asano T. A new high-T_c oxide superconductor without a rare earth element. Jpn J Appl Phys. 1988; 27:L209–10.
2. Ozturk O, Yegen D, Yilmazlar M, Varilci A, Terzioglu C. The effect of cooling rates on properties of $Bi_{1.7}Pb_{0.35}Sr_{1.9}Ca_{2.1}Cu_3O_y$ superconductors produced by solid-state reaction method. Phys C Supercond. 2007; 451(2):113–7.
3. Michel C, Hervieu M, Borel MM, Grandin A, Deslandes F, Provost J, Raveau B. Superconductivity in the Bi - Sr - Cu - O system. Z Phys B. 1987; 68(4):421–3.
4. Gul IH, Rehman MA, Ali M, Maqsood A. Effect of vanadium and barium on the Bi-based(2223) superconductors. Phys C Supercond. 2005; 432(1-2):71–80.
5. Lin Z, Persson M. Crystallisation and superconductivity of rapidly quenched (amorphous) Bi-Ca-Sr-Cu-O samples. Supercond Sci Technol. 1988; 1:198–200.
6. Xi Z, Ji C, Zhou L. 112–114 K superconductors $Bi_{1.8}Pb_{0.3}Sr_2Ca_2Cu_3O_y$ by means of a three-step reaction process. Solid State Commun. 1989; 72(10):1015–17.
7. Zhigadlo ND, Petrashko VV, Semenenko Yu A, Panagopoulos C, Cooper JR, Salje EKH. The effects of Cs doping, heat treatments on the phase formation and superconducting properties of (Bi, Pb)–Sr–Ca–Cu–O ceramics. Phys C Supercond. 1998; 299(3–4):327–37.
8. Gul IH, Anis-ur-Rehman M, Maqsood A. Temperature dependence of thermal and electrical conductivity of Bi-based high-T_c (2223) superconductor. Phys C Supercond. 2006; 450(1–2):83–7.
9. Li Y, Yang B. Doping of the Bi-Sr-Ca-Cu-O system with V_B elements and the effect on $Bi_2Sr_2Ca_2Cu_3O_y$ phase formation. J Mater Sci Lett. 1994; 13(8):594–6.

10. Salamati H, Kameli P. The effect of Bi-2212 phase on the weak link behavior of Bi-2223 superconductors. Phys C Supercond. 2004; 403(1–2):60–6.
11. Ghazanfaria N, Kilic A, Gencerb A, Ozkana H. Effects of Nb_2O_5 addition on superconducting properties of BSCCO. Solid State Comm. 2007; 144(5–6):210–4.
12. dos Santos CAM, Mochlecke S, Kopelevich Y, Machado AJS. In homogeneous superconducting in $Bi_2Sr_2Ca_{1-x}Pr_xCu_2O_{8-z}$. Phys C Supercond. 2003; 390(1):21–6.
13. Rentschler T, Kemmler-Sack S, Hartmann M, Hubenen RP, Kesselar P, Lichte H. Influence of Nd substitution on the superconducting properties of ceramics in the 2212 System $Bi_{2-w}Pb_wSr_{2-y}Nd_{x+y}Cu_xO_{8+z}$. Phys C Supercond. 1992; 200(3–4):287–95.
14. Biju A, Abhilash Kumar RG, Aloysius RP, Syamaprasad U. Structual and superconducting properties of $Bi_{1.7}Pb_{0.4}Sr_{2-x}Gd_xCa_{1.1}Cu_2O_y$. Phys C Supercond. 2006; 449(2):109–15.
15. Awana VPS, Agarawal SK, Narlikar AV, Das MP. Superconductivity in Pr- and Ce-Doped $Bi_2CaSr_2Cu_2O_y$ system. Phys Rev B. 1993; 48(2):1211–16.
16. Berger H, Ariosa D, Gaal R, Saleh A, Margaritondo G, Lee SF, Huang SH, Chang HW, Chuang TM, Liou Y, Yao YD, Hwu Y. Coexistance of ferromagnetism and high-temperature superconductivity in Dy-Doped BiPbSrCaCuO. Surf Rev Lett. 2002; 9(2):1109–112.
17. Zelati A, Amirabadizadeh A, Kompany A, Salamati H, Sonier J. Manufacture and characterization of Dy_2O_3 nano-particles via X-ray diffraction, TEM and PL. Indian J Sci Technol. 2013; 6(12):5552–58.
18. Nabil AA. Yahya, Abd-Shukor R. Effect of different nano-sized MgO on the transport critical current density of $Bi_{1.6}Pb_{0.4}Sr_2Ca_2Cu_3O_{10}$ superconductor. J Supercond Nov Magn. 2013 Jul; 27(2):329–35. doi: 10.1007/s10948-013-2302-5
19. Mawassi R, Marhaba S, Roumié M, Awad R, Korek M, Hassan I. Improvement of superconducting parameters of $Bi_{1.8}Pb_{0.4}Sr_2Ca_2Cu_3O_{10+\delta}$ added with nano-Ag. J Supercond Nov Magn. 2013 Nov. doi: 10.1007/s10948-013-2408-9.
20. Kong W, Abd-Shukor R. Enhanced electrical transport properties of nano $NiFe_2O_4$ added $(Bi_{1.6}Pb_{0.4})$ $Sr_2Ca_2Cu_3O_{10}$ superconductor. Journal of Superconductivity and Novel Magnetism. 2010; 23(2): 257–63.
21. Agail A, Abd-Shukor R. Transport current density of $(Bi_{1.6}Pb_{0.4})Sr_2Ca_2Cu_3O_{10}$ superconductor added with different nano-sized ZnO. Appl Phys A. 2013; 112(2): 501–6.
22. Mao C, Zhou L, Wu X, Sun X. The combination of the polymeric solution-sol-gel process and combustion synthesis to manufacture BiPbSrCaCuO powder. Supercond Sci Technol. 1996; 9:994–1000.
23. Tampieri A, Celotti G, Lesca S, Bezzi G, La Torretta TMG, Magnani G. Bi(Pb)-Sr-Ca-Cu-O (2223) superconductor prepared by improved sol-gel technique. J Eur Ceram Soc. 2000; 20(2):119–26.
24. Halim SA, Khawaldeh SA, Mohamed SB, Azhan H. Superconducting properties of $Bi_{2-x}Pb_xSr_2Ca_2Cu_3O_y$ system derived via sol-gel and solid state routes. Mater Chem Phys. 1999; 61(3):251–9.
25. Saleh SA. Studies on sintering effect on the structural and transport properties of (2223) phase. Phys C Supercond. 2006; 444(1–2):40–4.
26. Mia S, Balanetskyya S, Grushkoa B. A study of the Al-rich part of the Al–Ru alloy system. Intermetallics. 2003; 11(7):643–9.
27. He HP, Huang XJ, Chen LQ. An effective way to detect the secondary phase in Sr-doped $LaInO_3$. J Phys Chem Solid. 2001; 62(4):701–9.
28. Kocabas K, Ciftcioglu M. The effect of Sb substitution of Cu in $Bi_{1.7}Pb_{0.3}Sr_2Ca_2Cu_{3-x}Sb_xO_y$ superconductors. Phys. Stat Sol. (a). 2000; 177(2):539–45.
29. Bilgili O, Selamet Y, Kocabas K. Effects of Li substitution in Bi-2223 superconductors. J Supercond Nov Magn. 2008; 21(8): 439–49.
30. Bean CP. Magnetization of high-field superconductors. Rev Modern Phys. 1964; 36(1):31–9.